2019 American Control Conference (ACC)
Philadelphia, PA, USA, July 10-12, 2019

Adaptive Feedback Noise Control for Wide, Square, and Tall Systems

Antai Xie and Dennis S. Bernstein

Abstract— **This paper considers MIMO feedback noise control in a three-dimensional acoustic space, where the plant may be wide, tall, or square. The goal is to investigate the implications of the plant aspect ratio within the context of retrospective cost adaptive control (RCAC), which is susceptible to canceling unmodeled nonminimum-phase transmission zeros. To obtain the necessary modeling information, each control speaker is impulsed, and the data from the resulting impulse response is used to construct the intercalated target model needed by RCAC. No additional system identification or analytical modeling is used for controller implementation. Laboratory experiments are used to evaluate the ability of RCAC to reject disturbances for wide, square, and tall sensor/actuator configurations.**

I. INTRODUCTION

The paradox of feedback control is that feedback reduces the need for an accurate model of the plant dynamics, but an inaccurate model can lead to poor performance and possibly instability. The traditional approach tox feedback control in the face of model uncertainty is robust control, where the controller is designed to provide robust stability and performance over the set of possible plants. Robust control thus requires a set of models (usually characterized by a nominal model and uncertainty bounds) that is guaranteed to include the true plant or, at least, a nominal plant model that is sufficiently close to the true plant so that the residual model error has minimal adverse impact on stability and performance.

In practice, constructing a set of models that captures the true plant can require substantial effort. Furthermore, designing a controller that provides robust stability and performance for all models in the set means that the achievable performance is hampered by the need to account for the least accurate model in the set. In extreme cases, the uncertainty in the plant may be so severe that there exists no feasible controller that can deliver acceptable performance over the entire uncertainty set. In addition, if the plant changes in an unanticipated way due to aging, faults, or damage, then it may be extremely difficult if not impossible to construct a useful set of models that includes the true plant. These challenges motivate the need for adaptive control

Adaptive control algorithms have been developed for both feedback and feedforward control architectures. In particular, adaptive feedforward algorithms have been extensively developed for acoustic noise control [1], [2], [3], [4], [5], [6]. Feedforward control is feasible for this application due to the fact that, in many cases, a disturbance measurement that is not corrupted by the control input is available. Furthermore, in narrowband applications, this requirement can be relaxed to knowing only the frequency of the disturbance, from which the time-domain signal can be synthesized [7]. Unlike feedback control, feedforward control cannot stabilize the plant. Therefore, feedforward control is confined to asymptotically stable systems such as acoustic noise control. Furthermore, in order to avoid the possibility of plant destabilization, feedforward control requires that the controller remain asymptotically stable.

The present paper focuses on feedback noise control in cases where feedforward control is not implementable [8], [9]. This situation occurs in the case where measurements of the disturbance that are not corrupted by the control input are not available. For example, in the case of road noise, measurements from microphones located inside the vehicle are corrupted by the control signal from the control speakers. Consequently, feedforward control requires that microphones or accelerometers be located outside the vehicle; however, this adds signal delay and complexity due to sensor placement. In contrast, feedback control can be used directly with interior microphones.

In cases where feedforward control is not feasible for noise control, feedback control must be considered [10], [11]. However, as mentioned above, feedback control risks instability and thus may require a more detailed model than feedforward control. In addition, unlike feedforward control, the achievable performance of a feedback controller is limited by the Bode integral constraints on the sensitivity function [12], [13].

In many applications of feedback noise control, detailed modeling of the acoustic space is impractical. For example, modeling the interior of a car requires complete geometry of the seats and dashboard, the reflectivity of the materials of all surfaces, the geometry of the occupants of the vehicle, and the state of all windows (partially or fully open or closed). Small changes in any of these features—which can change significantly and unpredictably over time—can severely affect the modal frequencies and mode shapes. An acoustic model of this system obtained by either identification or physics modeling is inevitably worthless in practice.

The difficulty in modeling acoustic dynamics for feedback control motivates the need for adaptive feedback control techniques that are applicable to broadband disturbance rejection. To address this need, the present paper considers retrospective cost adaptive control (RCAC). In [14], RCAC was applied to feedback noise control in a duct, and, more recently, to noise control in a car [15]. A recent overview of

The authors are with the Department of Aerospace Engineering, University of Michigan, Ann Arbor, MI 48109.

978-1-5386-7928-9/$31.00 ©2019 AACC

RCAC is given in [16].

For linear SISO systems, RCAC requires information about the leading sign, relative degree, and nonminimum-phase (NMP) zeros. This information is incorporated in the target model G_{f}, which is used to define the retrospective cost. As discussed in [16], G_{f} serves as a target model for the closed-loop intercalated transfer function from the virtual control input perturbation to the performance variable. Since open-loop zeros are unmoved by feedback, these zeros also appear in the closed-loop intercalated transfer function. Consequently, if a NMP zero of the plant is not included in G_{f}, RCAC may cancel the zero in attempting to match the closed-loop intercalated transfer function to G_{f}.

The goal of the present paper is to investigate the feasibility of applying RCAC to feedback noise control with multiple speakers and microphones. A key objective of this paper is to investigate the modeling information needed to construct the target model in MIMO case. Unlike the SISO case, where the leading sign, relative degree, and nonminimum-phase (NMP) zeros are relative easy to characterize, these features are difficult to define and estimate in the MIMO case. For example, in order to avoid unstable pole-zero cancellation, it is necessary to identify the input and output directions of each NMP transmission zero. In practice it is difficult to obtain this modeling information; in fact, as discussed above, small changes in the acoustic space geometry would likely render this information invalid, thus risking NMP transmission zero cancellation.

With these challenges in mind, the present paper addresses the MIMO feedback noise control problem by using the measured impulse response to construct the MIMO target model. In particular, we impulse each control input and measure the resulting impulse response. By combining the impulse responses across all input channels, we construct the target model G_{f}. It follows from properties of the Laurent expansion that the resulting target model includes an approximate model of the plant NMP zeros and associated zero directions. The underlying goal is to determine whether the modeling information required by RCAC can be obtained with an extremely limited amount of data without analytical modeling or additional system identification.

To investigate the feasibility of this approach, we perform feedback noise control experiments involving. The experiments include MIMO plants that are wide (1 microphone and 2 speakers), square (2 microphone and 2 speakers), and tall (2 microphones and 2 speakers). We note that wide and tall plants generically have no zeros, and thus these plants are less susceptible to unstable pole-zero cancellation. The square case (which includes SISO plants) is potentially more difficult, since these systems may possess one or more NMP zero.

II. THE ADAPTIVE STANDARD AND SERVO PROBLEM

Consider the discrete-time, linear time-invariant standard control problem written using the time-domain forward-shift operator $\mathbf{q}$ given by

$$z_k = G_{zw}(\mathbf{q})w_k + G_{zu}(\mathbf{q})u_k, \tag{1}$$

$$y_k = G_{yw}(\mathbf{q})w_k + G_{yu}(\mathbf{q})u_k, \tag{2}$$

where $y_k \in \mathbb{R}^{l_y}$ is the measurement, $u_k \in \mathbb{R}^{l_u}$ is the control input, $w_k \in \mathbb{R}^{l_w}$ is the exogenous input, and $z_k \in \mathbb{R}^{l_z}$ is the measured performance variable. The components of w can represent either a command signal r to be followed, a disturbance d to be rejected, or sensor noise v that corrupts the measurements. The plant (1) and (2) may represent a continuous-time, linear time-invariant plant sampled at a fixed rate. As a special case of the standard problem, the servo problem is given as

$$w = \begin{bmatrix} r & d & v \end{bmatrix}^{\mathrm{T}}, \quad y = z, \tag{3}$$

$$G_{zw} = G_{yw} = \begin{bmatrix} I_{l_y} & -G_d & -I_{l_y} \end{bmatrix}, \tag{4}$$

$$G_{zu} = G_{yu} = -G_u. \tag{5}$$

We define the signal y_0 as

$$y_{0,k} = G_d(\mathbf{q})d_k + G_u(\mathbf{q})u_k, \tag{6}$$

where, if $z = y = 0$, then $y_0 = r$. The control input u is given by the linear, time-varying dynamic compensator $G_{\mathrm{c},k}$, where

$$u_k = G_{\mathrm{c},k}(\mathbf{q})y_k \tag{7}$$

III. CONTROLLER STRUCTURE

We consider a dynamic compensator $G_{\mathrm{c},k}$ of the form

$$u_k = \sum_{i=1}^{n_{\mathrm{c}}} P_k(i)u_{k-i} + \sum_{j=k_{\mathrm{c}}}^{n_{\mathrm{c}}} Q_k(j)y_{k-j}, \tag{8}$$

where $P_k(i) \in \mathbb{R}^{l_u \times l_u}$ and $Q_k(j) \in \mathbb{R}^{l_u \times l_y}$ are time-dependent controller coefficient matrices, n_{c} is the controller order, and $k_{\mathrm{c}} \geq 0$. For controller startup, we implement (8) as

$$u_k = \begin{cases} 0, & k < k_{\mathrm{w}}, \\ \Phi_k\theta_k, & k \geq k_{\mathrm{w}}, \end{cases} \tag{9}$$

where the regressor matrix Φ_k is defined by

$$\Phi_k \triangleq \begin{bmatrix} u_{k-1} \\ \vdots \\ u_{k-n_{\mathrm{c}}} \\ y_{k-k_{\mathrm{c}}} \\ \vdots \\ y_{k-n_{\mathrm{c}}} \end{bmatrix}^{\mathrm{T}} \otimes I_{l_u} \in \mathbb{R}^{l_u \times l_\theta}, \tag{10}$$

$k_{\mathrm{w}} \geq n_{\mathrm{c}}$ is an initial waiting period during which Φ_k is populated with data, and the controller coefficient vector θ_k is defined by

$$\theta_k \triangleq \operatorname{vec}\begin{bmatrix} P_k(1) & \cdots & P_k(n_{\mathrm{c}}) & Q_k(k_{\mathrm{c}}) & \cdots & Q_k(n_{\mathrm{c}}) \end{bmatrix} \in \mathbb{R}^{l_\theta}, \tag{11}$$

$l_\theta \triangleq l_u^2 n_\mathrm{c} + l_u l_y (n_\mathrm{c}+1-k_\mathrm{c})$, "$\otimes$" is the Kronecker product, and "vec" is the column-stacking operator. k_c determines the relative degree of the controller, where we typically choose $k_\mathrm{c} \geq 1$. We can write (7) in terms of $P_k(i)$ and $Q_k(j)$ as

$$G_{\mathrm{c},k} = D_{\mathrm{c},k}^{-1} N_{\mathrm{c},k} \tag{12}$$

where

$$D_{\mathrm{c},k} = I_{l_u}\mathbf{q}^{n_\mathrm{c}} - P_k(1)\mathbf{q}^{n_\mathrm{c}-1} - \cdots - P_k(n_\mathrm{c}), \tag{13}$$

$$N_{\mathrm{c},k} = Q_k(k_\mathrm{c})\mathbf{q}^{n_\mathrm{c}-k_\mathrm{c}} + \cdots + Q_k(n_\mathrm{c}). \tag{14}$$

In this paper, we consider a *super-sparse* parameterization of $D_{\mathrm{c},k}$ such that

$$D_{\mathrm{c},k}(\mathbf{q}) = d_{\mathrm{c},k}(\mathbf{q}) I_{l_\mathrm{u}}, \tag{15}$$

and

$$u_k = \sum_{i=1}^{n_\mathrm{c}} p_k(i) u_{k-i} + \sum_{j=k_\mathrm{c}}^{n_\mathrm{c}} Q_k(j) y_{k-j}. \tag{16}$$

where $p_k(i)$ are scalars. It follows that (10) and (11) are given by

$$\Phi_k = \begin{bmatrix} \Phi_{u,k} & \Phi_{y,k} \end{bmatrix}, \quad \theta_k = \begin{bmatrix} \theta_{u,k} \\ \theta_{y,k} \end{bmatrix}, \tag{17}$$

where

$$\Phi_{u,k} = \begin{bmatrix} u_{k-1} & \cdots & u_{k-n_\mathrm{c}} \end{bmatrix}, \quad \Phi_{y,k} = \begin{bmatrix} y_{k-k_\mathrm{c}} \\ \vdots \\ y_{k-n_\mathrm{c}} \end{bmatrix}^{\mathrm{T}} \otimes I_{l_u}, \tag{18}$$

$$\theta_{u,k} = \begin{bmatrix} p_k(1) \\ \vdots \\ p_k(n_\mathrm{c}) \end{bmatrix}, \quad \theta_{y,k} = \operatorname{vec}\begin{bmatrix} Q_k(k_\mathrm{c}) & \cdots & Q_k(n_\mathrm{c}) \end{bmatrix}, \tag{19}$$

and $l_\theta = n_\mathrm{c} + l_u l_y (n_\mathrm{c} + 1 - k_\mathrm{c})$.

IV. RETROSPECTIVE COST ADAPTIVE CONTROL

Define the *retrospective performance variable* as

$$\hat{z}(k,\hat{\theta}) \triangleq z_k - G_\mathrm{f}(\mathbf{q})u_k - G_\mathrm{f}(\mathbf{q})\Phi_k\hat{\theta}, \tag{20}$$

where $\hat{\theta} \in \mathbb{R}^{l_\theta}$ and the $n_z \times n_u$ filter G_f has the form

$$G_\mathrm{f} \triangleq D_\mathrm{f}^{-1} N_\mathrm{f}, \tag{21}$$

D_f is an $l_z \times l_z$ polynomial matrix with leading coefficient I_{l_z}, and N_f is an $l_z \times l_u$ polynomial matrix. The filter G_f serves as the *target model*, as described in the next section. By defining the filtered regressor and filtered control $\Phi_{\mathrm{f},k} \in \mathbb{R}^{l_z \times l_\theta}$ and $u_{\mathrm{f},k} \in \mathbb{R}^{l_z}$ by

$$\Phi_{\mathrm{f},k} \triangleq G_\mathrm{f}(\mathbf{q})\Phi_k, \quad u_{\mathrm{f},k} \triangleq G_\mathrm{f}(\mathbf{q})u_k, \tag{22}$$

(20) can be written as

$$\hat{z}(k,\hat{\theta}) = z_k - u_{\mathrm{f},k} - \Phi_{\mathrm{f},k}\hat{\theta}. \tag{23}$$

Define the *cumulative retrospective cost function* as

$$\begin{aligned} J_\mathrm{C}(k,\hat{\theta}) \triangleq{}& \sum_{i=1}^{k} \lambda^{k-i} \hat{z}^{\mathrm{T}}(i,\hat{\theta}) R_z \hat{z}(i,\hat{\theta}) \\ &+ \sum_{i=1}^{k} \lambda^{k-i} (\Phi_{\mathrm{f},i}\hat{\theta})^{\mathrm{T}} R_{u_\mathrm{f}} \Phi_{\mathrm{f},i}\hat{\theta} \\ &+ \sum_{i=1}^{k} \lambda^{k-i} (\Phi_i\hat{\theta})^{\mathrm{T}} R_u \Phi_i\hat{\theta} \\ &+ (\hat{\theta}-\theta_{k-1})^{\mathrm{T}} R_\Delta (\hat{\theta}-\theta_{k-1}) \\ &+ \lambda^k (\hat{\theta}-\theta_0)^{\mathrm{T}} R_\theta (\hat{\theta}-\theta_0), \end{aligned} \tag{24}$$

where $\lambda \in (0,1]$ is the forgetting factor, $R_\theta \in \mathbb{R}^{l_\theta \times l_\theta}$ and $R_z \in \mathbb{R}^{l_z \times l_z}$ are positive definite, and $R_{u_\mathrm{f}} \in \mathbb{R}^{l_z \times l_z}$ $R_u \in \mathbb{R}^{l_u \times l_u}$, and R_Δ are positive semidefinite. Note that the weights in (24) can be chosen to be time-varying, however in this paper, we assume them to be constant. Define the augmented weight and regressor matrices

$$R_\mathrm{a} \triangleq \begin{bmatrix} R_z + R_{u_\mathrm{f}} & 0_{l_z \times l_u} \\ 0_{l_u \times l_z} & R_u \end{bmatrix}, \tag{25}$$

$$R_\mathrm{a}' \triangleq \begin{bmatrix} R_z & 0_{l_z \times l_u} \\ 0_{l_u \times l_z} & R_u \end{bmatrix}, \tag{26}$$

$$\Phi_{\mathrm{a},k} \triangleq \begin{bmatrix} \Phi_{\mathrm{f},k} \\ \Phi_k \end{bmatrix}, \quad z_{\mathrm{a},k} \triangleq \begin{bmatrix} z_k - u_{\mathrm{f},k} \\ 0_{l_u \times 1} \end{bmatrix}. \tag{27}$$

Proposition: Let $P_0 = R_\theta^{-1}$, $k \geq 1$, and the weights (25)–(27) be constant. Denote $\hat{\theta}^*$ as the minimizer of (24) at step k. Then,

$$\begin{aligned} \hat{\theta}^* = \theta_k &- P_k \Phi_{\mathrm{a},k}^{\mathrm{T}} \Upsilon_k^{-1} \epsilon_k \\ &+ P_k R_\Delta [\Phi_{\mathrm{a},k}^{\mathrm{T}} \Upsilon_k^{-1} \Phi_{\mathrm{a},k} P_k - I_{l_\theta}](\theta_{k-1} - \theta_k), \end{aligned} \tag{28}$$

where

$$\Upsilon_k \triangleq \lambda R_\mathrm{a}^{-1} + \Phi_{\mathrm{a},k} P_k \Phi_{\mathrm{a},k}^{\mathrm{T}}, \tag{29}$$

$$\epsilon_k \triangleq \Phi_{\mathrm{a},k}\theta_k + R_\mathrm{a}^{-1} R_\mathrm{a}' z_{\mathrm{a},k} \tag{30}$$

and P_k satisfies

$$P_{k+1} = \frac{1}{\lambda} P_k - \frac{1}{\lambda} P_k \Phi_{\mathrm{a},k}^{\mathrm{T}} \Upsilon_k^{-1} \Phi_{\mathrm{a},k} P_k. \tag{31}$$

Setting $\theta_{k+1} = \hat{\theta}^*$ yields the recursive controller coefficient update

$$\begin{aligned} \theta_{k+1} = \theta_k &- P_k \Phi_{\mathrm{a},k}^{\mathrm{T}} \Upsilon_k^{-1} \epsilon_k \\ &+ P_k R_\Delta [\Phi_{\mathrm{a},k}^{\mathrm{T}} \Upsilon_k^{-1} \Phi_{\mathrm{a},k} P_k - I_{l_\theta}](\theta_{k-1} - \theta_k). \end{aligned} \tag{32}$$

If R_u is not positive definite, then R_a^{-1} is replaced by its pseudoinverse.

V. MIMO TARGET MODEL G_f

Substituting $\hat{\theta} = \theta_{k+1}$, (20) can be written as

$$\hat{z}(k,\theta_{k+1}) = z_k - G_\mathrm{f}(\mathbf{q})[u_k - \Phi_k \theta_{\overline{k+1}}] \tag{33}$$

where $\theta_{\overline{k+1}}$ indicates that $G_\mathrm{f}(\mathbf{q})$ operates on Φ_k but not on θ_{k+1}. This restriction arises from the fact that, in the defi-

nition (20) of $\hat{z}(k,\hat{\theta})$, $\hat{\theta}$ is a constant that is not affected by $G_{\rm f}(\mathbf{q})$. By defining the *virtual external control perturbation*

$$\tilde{u}(k,\hat{\theta}) \triangleq u_k - \Phi_k\hat{\theta}, \tag{34}$$

(33) can be written as

$$\hat{z}(k,\theta_{k+1}) = z_k - G_{\rm f}(\mathbf{q})\tilde{u}(k,\theta_{\overline{k+1}}). \tag{35}$$

Rewriting u_k in terms of $\tilde{u}(k,\theta_{\overline{k+1}})$, we obtain

$$\begin{aligned} u_k &= \tilde{u}(k,\theta_{\overline{k+1}}) + \Phi_k\theta_{k+1} \\ &= \tilde{u}(k,\theta_{\overline{k+1}}) + \sum_{i=1}^{n_{\rm c}} P_{k+1}(i)u_{k-i} + \sum_{j=k_{\rm c}}^{n_{\rm c}} Q_{k+1}(j)y_{k-i}, \end{aligned} \tag{36}$$

which can be rewritten as

$$\begin{aligned} \left(I_{l_u} - \sum_{i=1}^{n_{\rm c}} P_{k+1}(i)\frac{1}{\mathbf{q}^i}\right) u_k &= \tilde{u}(k,\theta_{\overline{k+1}}) \\ &\quad + \left(\sum_{j=k_{\rm c}}^{n_{\rm c}} Q_{k+1}(j)\frac{1}{\mathbf{q}^i}\right) y_k. \end{aligned} \tag{37}$$

Introduce the notation

$$D_{{\rm c},\hat{\theta}}(\mathbf{q}) \triangleq \mathbf{q}^{n_{\rm c}}I_{l_u} - \mathbf{q}^{n_{\rm c}-1}\hat{P}(1) - \cdots - \hat{P}(n_{\rm c}), \tag{38}$$

$$N_{{\rm c},\hat{\theta}}(\mathbf{q}) \triangleq \mathbf{q}^{n_{\rm c}-k_{\rm c}}\hat{Q}(k_{\rm c}) + \cdots + \hat{Q}(n_{\rm c}). \tag{39}$$

In the subsequent derivation in this section, we drop the implicit $\theta_{\overline{k+1}}$ in all transfer function subscripts, where, for example, it is assumed that

$$D_{{\rm c},\theta_{k+1}}(\mathbf{q}) = D_{{\rm c},\theta_{\overline{k+1}}}(\mathbf{q}). \tag{40}$$

Using the notation (38) and (39), (37) can be written as

$$u_k = G_{{\rm p},\theta_{k+1}}(\mathbf{q})\tilde{u}(k,\theta_{\overline{k+1}}) + G_{{\rm c},\theta_{k+1}}(\mathbf{q})y_k, \tag{41}$$

where

$$G_{{\rm c},\theta_k} \triangleq D_{{\rm c},\theta_k}^{-1}N_{{\rm c},\theta_k}, \tag{42}$$

$$G_{{\rm p},\theta_k} \triangleq D_{{\rm c},\theta_k}^{-1}\mathbf{q}^{n_{\rm c}}. \tag{43}$$

Substituting (41) into (1), (2), we can write z_k in terms of $u(k,\theta_{\overline{k+1}})$ as

$$z_k = \tilde{G}_{zw,\theta_{k+1}}(\mathbf{q})w_k + \tilde{G}_{z\tilde{u},\theta_{k+1}}(\mathbf{q})\tilde{u}(k,\theta_{\overline{k+1}}), \tag{44}$$

where

$$\tilde{G}_{zw,\theta_k} \triangleq G_{zw} + G_{zu}G_{{\rm c},\theta_k} \tag{45}$$

$$(I_{ly} - G_{yu}G_{{\rm c},\theta_k})^{-1}G_{yw}, \tag{46}$$

$$\tilde{G}_{z\tilde{u},\theta_k} \triangleq G_{zu}(I_{lu} - G_{{\rm c},\theta_k}G_{yu})^{-1}G_{{\rm p},\theta_k}. \tag{47}$$

Substituting (44) into (35), it follows that the retrospective performance $\hat{z}(k,\theta_{k+1})$ can be written as

$$\hat{z}(k,\theta_{k+1}) = \hat{z}_{\rm pp}(k,\theta_{k+1}) + \hat{z}_{\rm mm}(k,\theta_{k+1}), \tag{48}$$

where $\hat{z}_{\rm pp}$ is the *pseudo-performance*

$$\hat{z}_{\rm pp}(k,\theta_{k+1}) = \tilde{G}_{zw,\theta_{k+1}}(\mathbf{q})w(k), \tag{49}$$

which is the performance of the system assuming that the updated controller coefficient vector θ_{k+1} had been used at step k, and $\hat{z}_{\rm mm}$ is the *model-matching error*

$$\hat{z}_{\rm mm}(k,\theta_{k+1}) = [\widetilde{G}_{z\tilde{u},\theta_{k+1}}(\mathbf{q}) - G_{\rm f}(\mathbf{q})]\tilde{u}(k,\theta_{\overline{k+1}}), \tag{50}$$

which is the residual between between the filter $G_{\rm f}$ and $\widetilde{G}_{z\tilde{u},\theta_{k+1}}$ subject to the virtual external control perturbation $\tilde{u}(k,\theta_{\overline{k+1}})$. The observation that model-matching term can be viewed as a residual between $G_{\rm f}$ and $\widetilde{G}_{z\tilde{u},\theta_{k+1}}$ leads to the conclusion that $G_{\rm f}$ needs to capture certain properties of $\widetilde{G}_{z\tilde{u},\theta_{k+1}}$ and guides filter design.

In [16] it was shown in the SISO case that $G_{\rm f}$ needs to capture the first nonzero Markov parameter, relative degree, and NMP zeros of $\widetilde{G}_{z\tilde{u},\theta_{k+1}}$. From (47), it was determined that the first nonzero Markov parameter, relative degree, and NMP zeros of $\widetilde{G}_{z\tilde{u},\theta_{k+1}}$ are the same in G_{zu}. Hence the modeling information can be obtained from the open-loop transfer function G_{zu}.

In this paper, we use the Markov parameters of G_{zu} to obtain the necessary model information for the target model in the MIMO case. In particular, for each complex number $\mathbf{z}$ whose absolute value is greater than the spectral radius of G_{zu},

$$G_{zu}(\mathbf{z}) = H_0 + \sum_{i=1}^{\infty}\frac{H_i}{\mathbf{z}^i} \tag{51}$$

where the Markov parameters $H_0, H_1, H_3, \ldots,$ are the impulse-response coefficients. Alternatively, in terms of a state-space realization (A,B,C,D) of G_{zu},

$$H_0 = D, \quad H_i = CA^{i-1}B. \tag{52}$$

For an asymptotically stable system, the Markov Parameters are convergent, and we can obtain an approximation of G_{zu} by truncating the Laurent series (51). We choose $G_{\rm f}$ as

$$G_{\rm f} = H_0 + \sum_{i=1}^{n_{\rm f}}\frac{H_i}{\mathbf{z}^i}, \tag{53}$$

where, for sufficiently large $n_{\rm f}$, the invariant NMP zeros and relative degree of G_{zu} are captured. If G_{zu} is not asymptotically stable, then the sequence of Markov parameters does not converge, and thus truncation of the series does not provide a useful estimate of G_{zu}.

VI. EXPERIMENTAL SETUP

We apply RCAC to an acoustic experiment using a dSPACE DS1104 board. Omni-directional microphones are used for sensing, and mid-bass woofers are used for actuation. Additional hardware includes speaker amplifiers, microphone amplifiers, and lowpass anti-aliasing filters. The controller is implemented at 500 Hz, and all signals are sampled at the same rate. A diagram of the microphone and speaker placement is shown in Figure 1. One speaker is chosen as the disturbance w, and two locations are considered for the control speakers u_1 and u_2. Three locations are considered for the performance microphone z, denoted as m_1, m_2, and m_3.

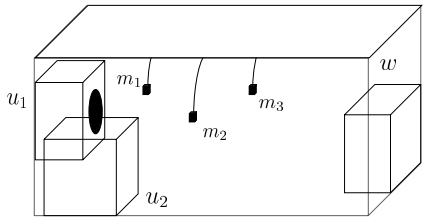

Fig. 1. Sensor and actuator placement in the acoustic experiment. The approximate dimensions of the enclosure are 6 ft × 3 ft × 3 ft.

VII. CONSTRUCTING THE TARGET MODEL G_{f}

We construct the Markov-parameter-based filter (53) using the impulse response from each speaker to microphone pair. Figure 2 shows the impulse response from s_1 to m_3. As sensor noise corrupts the leading Markov parameters

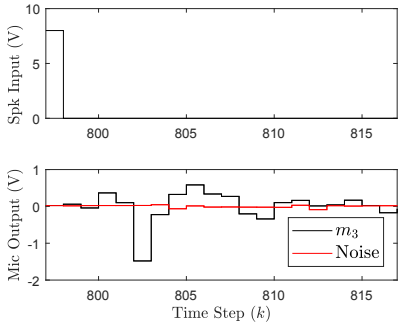

Fig. 2. Impulse response of s_1 to m_3. In order to improve the signal-to-noise ratio, we use an impulse of magnitude 8.

obtained from the impulse response, spurious zeros may appear in the resulting G_{f}. Hence, we modify the filter by zeroing the leading Markov parameters whose magnitude is below a chosen cutoff level. Figure 3 shows the truncated Laurent expansion of the unmodified and modified filter, where spurious zeros in the unmodified filter are eliminated in the modified filter.

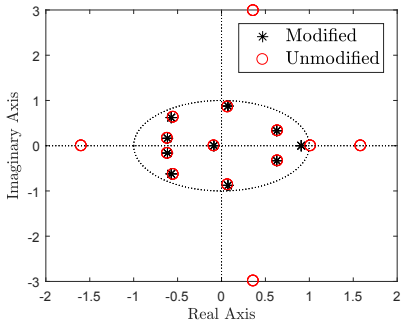

Fig. 3. Zeros of the truncated Laurent expansion of the unmodified and modified impulse response. In the modified impulse response, the leading coefficients below the noise floor are replaced by zeros. This removes four spurious zeros.

VIII. RCAC IMPLEMENTATION

RCAC is implemented in three configurations, namely, in cases where G_{zu} is wide, square, and tall. Let $r = 0$, and let w be given by

$$w_k = \sin(2\pi 80k) + \sin(2\pi 100k), \tag{54}$$

which is a two-tone disturbance with harmonics at 80 Hz and 100 Hz. Unless otherwise specified, all experimental examples use $n_{\mathrm{f}} = 15$ and the tuning parameters $R_z = I_{l_z}$, $R_{u_{\mathrm{f}}} = 0$, $\lambda = 1$, $R_\theta = 10^{-1} I_{l_\theta}$, $R_\Delta = 0$, $R_u = 0$, $k_{\mathrm{c}} = 1$, and $N_{\mathrm{c}} = 12$. For each example, we show the transient response and compare the frequency content of the open-loop and asymptotic closed-loop microphone signals, that is, after the controller coefficients converge. 2500 data points sampled at 500 Hz are used to generate the frequency-response plots.

Example 2: Square System. Choose $u = \begin{bmatrix} u_1 & u_2 \end{bmatrix}^{\mathrm{T}}$ and $z = \begin{bmatrix} m_1 & m_2 \end{bmatrix}^{\mathrm{T}}$. Figure 4 shows the performance of RCAC for the square system. ◇

Example 3: Wide System. Choose $u = \begin{bmatrix} u_1 & u_2 \end{bmatrix}^{\mathrm{T}}$ and $z = m_2$. Figure 5 shows the performance of RCAC for the wide system. ◇

Example 4: Tall System. Choose $u = u_1$ and $z = \begin{bmatrix} m_1 & m_2 \end{bmatrix}^{\mathrm{T}}$. Figure 6 shows the performance of RCAC for the tall system. ◇

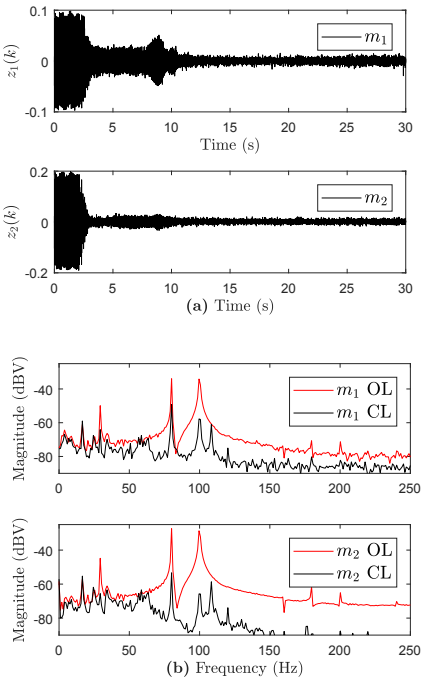

Fig. 4. Example 2: Performance of RCAC for the square system with $u = \begin{bmatrix} u_1 & u_2 \end{bmatrix}^{\mathrm{T}}$ and $z = \begin{bmatrix} m_1 & m_2 \end{bmatrix}^{\mathrm{T}}$. **(a)** shows the transient response of z, and the **(b)** shows the frequency content of the open-loop and asymptotic closed-loop z. Both disturbance frequencies are suppressed at both microphones.

IX. CONCLUSIONS AND FUTURE WORK

Retrospective cost adaptive control (RCAC) was experimentally applied to wide, square, and tall MIMO acoustic

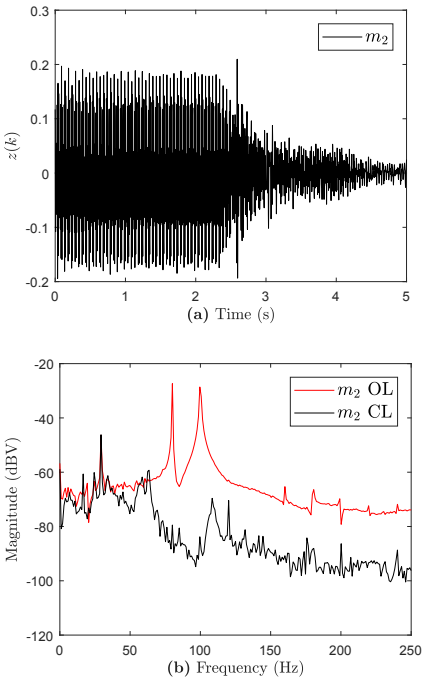

Fig. 5. Example 3: Performance of RCAC for the wide system with $u = \begin{bmatrix} u_1 & u_2 \end{bmatrix}^{\mathrm{T}}$ and $z = m_2$. **(a)** shows the transient response of z, and **(b)** shows the open-loop and asymptotic closed-loop frequency content of z. Both disturbance frequencies suppressed at m_2.

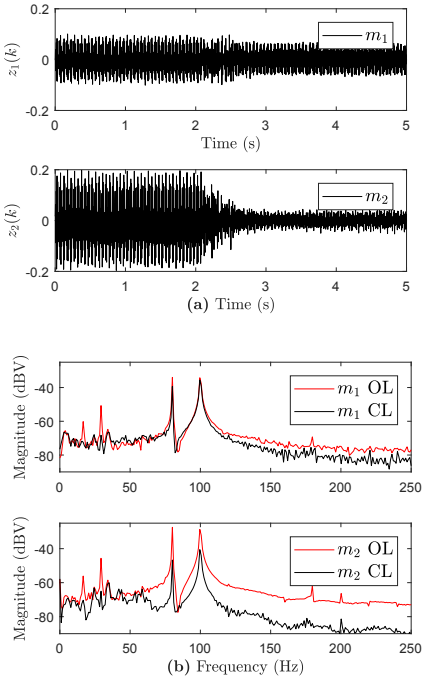

Fig. 6. Example 4: Performance of RCAC for the tall system with $u = u_1$ and $z = \begin{bmatrix} m_1 & m_2 \end{bmatrix}^{\mathrm{T}}$. **(a)** shows the transient response of z, and **(b)** shows the open-loop and asymptotic closed-loop frequency content of z. There is marginal suppression of the two disturbance frequencies at m_1 and partial suppression of both disturbance frequencies at m_2. This result is expected since the plant is tall.

plants. All modeling information was obtained by measuring the impulse response from the control speakers to the microphones. No knowledge of the spectrum or location of the disturbances was used. The results suggest that NMP transmission zeros are not present in the experimental setup. However, to the best of our knowledge, the existence or nonexistence of NMP transmission zeros in acoustic noise control applications remains an open research question. Future work focuses on the relationship between the target model G_{f} and $\tilde{G}_{z\tilde{u}}$ to better define the required modeling information required for RCAC in the MIMO case.

References

[1] J. C. Burgess, "Active adaptive sound control in a duct: A computer simulation," *J. Acous. Soc. Amer.*, vol. 70, no. 3, pp. 715–726, 1981.

[2] B. Widrow and S. D. Stearns, *Adaptive Signal Processing*. Prentice-Hall, 1985, vol. 15.

[3] S. Elliott, I. Stothers, and P. Nelson, "A multiple error lms algorithm and its application to the active control of sound and vibration," *IEEE Trans. Acous. Speech Sig. Proc.*, vol. 35, no. 10, pp. 1423–1434, Oct 1987.

[4] S. M. Kuo and D. R. Morgan, *Active Noise Control Systems: Algorithms and DSP Implementations*. Wiley, 1995.

[5] P. A. Nelson and S. J. Elliot, *Active Control of Sound*. Academic Press, 1992.

[6] C. Hansen, S. Snyder, X. Qiu, L. Brooks, and D. Moreau, *Active Control of Noise and Vibration*. CRC press, 2012.

[7] S. M. Kuo and D. R. Morgan, "Active Noise Control: A Tutorial Review," *Proc. IEEE*, vol. 87, no. 6, pp. 943–973, June 1999.

[8] L. A. Sievers and A. H. von Flotow, "Comparison and extensions of control methods for narrow-band disturbance rejection," *IEEE Trans. Sig. Proc.*, vol. 40, pp. 2377–2391, 1992.

[9] C. R. Fuller and A. H. von Flotow, "Active control of sound and vibration," *IEEE Contr. Sys. Mag.*, vol. 15, no. 6, pp. 9–19, 1995.

[10] S. M. Kuo, X. Kong, and W. S. Gan, "Applications of adaptive feedback active noise control system," *IEEE Trans. Contr. Sys. Tech.*, vol. 11, no. 2, pp. 216–220, 2003.

[11] J. Zeng and R. De Callafon, "Recursive filter estimation for feedforward noise cancellation with acoustic coupling," *J. Sound Vibr.*, vol. 291, no. 3-5, pp. 1061–1079, 2006.

[12] J. C. Doyle, B. A. Francis, and A. R. Tannenbaum, *Feedback Control Theory*. Macmillan, 1992.

[13] M. M. Seron, J. H. Braslavsky, and G. C. Goodwin, *Fundamental Limitations in Filtering and Control*. New York: Springer, 1997.

[14] R. Venugopal and D. S. Bernstein, "Adaptive Disturbance Rejection Using ARMARKOV/Toeplitz Models," *IEEE Trans. Contr. Sys. Tech.*, vol. 8, pp. 257–269, 2000.

[15] A. Xie and D. S. Bernstein, "Experimental investigation of spatial spillover in adaptive noise control of broadband disturbances in a 3D acoustic space," in *Proc. Amer. Contr. Conf.*, Boston, MA, July 2016, pp. 3410–3415.

[16] Y. Rahman, A. Xie, and D. S. Bernstein, "Retrospective Cost Adaptive Control: Pole Placement, Frequency Response, and Connections with LQG Control," *IEEE Contr. Sys. Mag.*, vol. 37, pp. 85–121, October 2017.